

## Research Paper

# A Histogram Separation and Mapping Framework for Image Contrast Enhancement

QIESHI ZHANG<sup>1,a)</sup> SEI-ICHIRO KAMATA<sup>1,b)</sup>

Received: February 12, 2012, Accepted: June 28, 2012, Released: September 18, 2012

**Abstract:** In this paper, an adaptive framework based on histogram separation and mapping for image contrast enhancement is presented. In this framework, the histogram is separated by binary tree structure with the proposed adaptive histogram separation strategy. Generally, histogram equalization (HE) is an effective technique for contrast enhancement. However, the conventional HE usually gives the processed image with unnatural look and artifacts by excessive enhancement. For overcoming this shortage, the adaptive histogram separation unit (AHSU) is proposed to convert the global enhancement problem into local. And for mapping the histogram partitions into more optimal ranges, the exact histogram separation is discussed. Finally, an adaptive histogram separation and mapping framework (AHSMF) for contrast enhancement is presented, and the experimental results show better effectiveness than other histogram based methods.

**Keywords:** image contrast enhancement, histogram separation, histogram mapping

## 1. Introduction

Image contrast enhancement plays a crucial role in image processing which allows various image contents/textures to be easily observed, such as, object detection and tracking, remote sensing, dynamic scene analysis, automatic navigation, biomedical image analysis, and other applications. However, there are several reasons to lead an image to poor contrast, such as, the poor quality of imaging device or the adverse conditions of acquisition, etc. In these situations, the captured image may not reveal all details of original scene, or have unnatural look. The image contrast enhancing technique aims to eliminate these problems for obtaining a more visually-pleasing and informative image. Therefore, several researchers have devoted their studies in this area. Histogram analysis is the most popular image processing procedure, and in this category histogram equalization (HE) is considered as a classical method. However, HE is less effective when the contrast characteristics vary across the image. To overcome this drawback, adaptive HE (AHE) [18] is proposed to generate the mapping of each pixel by the histogram in the surrounding partition. And many researchers, such as Stark [20] and Nilsson et al. [16], aim to improve this method in their studies. As well as HE based methods, the histogram specification (HS) based methods [9], [17], [19] and the transform based methods [2], [3], [21] were also studied.

Generally, the histogram based method is the main approach used to consider the relation of an image and its corresponding histogram. According to Arici et al. proposed method [5], a

cost function is composed of the image change and histogram deviation, forming the target and histogram smoothness. In histogram analysis based methods, HE and HS are the two major approaches, which are described as follows:

**HE based approach** aims to obtain a flat histogram to smoothen the gray level distribution. So based on AHE, Stark [20] proposed a HE generalization method. The main idea is to use the concise mathematical description of AHE and generate a mapping to estimate and convert the histogram. Beside Stark, Chen and Ramli [6] proposed the recursive mean-separate HE (RMSHE) to separate the histogram into  $2^l$  partitions, where  $l$  is the separation level. To achieve this, the histogram is separated into two partitions, which can be further separated into two sub-histogram partitions. And this procedure is repeated in  $l$  iteration which value needs to be set by user. Based on RMSHE, Nilsson et al. [16] proposed the successive mean quantization transform (SMQT) method to enhance the contrast. This separation method is similar to RMSHE but the selection of separation point is calculated by the mean quantization unit (MQU). Different from above, Kim et al. [13] proposed an overlapped sub-block based HE method to enable the histogram partitions to be equalized respectively. And Chen et al. [8] proposed an automatic enhancement approach by gray-level grouping (GLG). Also, Kim and Yang [14] interpolated the discrete probability density function (PDF) with Gaussian functions and applied nonlinear optimization. Additionally, Han et al. [11] recently proposed a 3-dimensional (3D) color HE method to define a new cumulative PDF in 3D color space.

**HS based approach** aims to transfer the histogram of an image into the histogram of another image to merge the characteristics of both histograms. Using the same idea with SMQT, Pei et al. [17] improved it and proposed a weighted histogram sep-

<sup>1</sup> Graduate School of Information, Production and Systems, Waseda University, Kitakyushu, Fukuoka 808–0135, Japan

a) q.zhang@akane.waseda.jp

b) kam@waseda.jp

aration (WHS) method. Also, Coltuc et al. [9] improved their previous work and proposed the exact HS (EHS) based on strict ordering among image pixels. After that, Sen and Pal [19] proposed an automatic EHS (AEHS) technique used for global and local contrast enhancement. With the same automatic strategy, Zhang et al. [25] proposed a binary tree structure based adaptive histogram separation to overcome the backlight influence of image.

In general, the HE based approach only focuses on the separation of histogram into several sub-partitions, allowing the partitions to become smooth. The HS based approach not only finds the separate solution but also devotes to determine the mapping function to obtain more results. Therefore, HS based methods can be considered as the enhanced HE approach.

To overcome the deficiency of HE based methods and improve HS based methods by separation point selection with adaptive judgment, we proposed an adaptive image contrast enhancement method using exact histogram adjustment technique. The adaptive histogram separation and mapping framework (AHSMF) is proposed to solve the separation point judgment and selection. For obtaining local details, the local contrast enhancement method is also studied. Lastly, the quantified evaluation of the effectiveness of contrast enhancement of the proposed method is demonstrated.

The rest of the paper is organized as follows: Section 2 introduces the definition of proposed AHSMF which is used to judge, separate, and map the histogram. Section 3 presents the local contrast enhancement approach. And experimental results, including the comparison with other methods, are provided in Section 4. Finally, conclusion is provided in the last section.

## 2. Adaptive Histogram Separation and Mapping Framework (AHSMF)

In this section, the proposed AHSMF is introduced in detail. To use the proposed framework for image contrast enhancement, the first step is to determine whether the current histogram partition needs to be separated for specification by the adaptive histogram separation unit (AHSU) or not. Considering that one gray value in a histogram may include several pixels, directly selecting the separate point in a histogram is not sufficient. Thus, the EHS is also studied in this section.

The main structure of AHSMF is shown in Fig. 1. AHSMF can separate the histogram into two partitions by AHSU recursive. In this framework,  $H_{i,j}$  is the current histogram partition, where  $i$  is the separation level, and  $j$  is the order of the current level. The partitions are mapped after the sub-histogram partition judgment and selection. Finally, the partitions are combined to a new histogram, and then the contrast enhanced image is obtained. AHSMF can be achieved in the following four steps:

**Step 1.** The current histogram or sub-histogram partition is judged whether it needs to be separated by AHSU or not. Repeat step 1 if need; otherwise, step 2 is performed.

**Step 2.** The sub-histogram partition is mapped into a new range.

**Step 3.** The sub-histogram partition is equalized independently.

**Step 4.** The new partitions are combined to form a new histogram and global brightness normalization is performed.

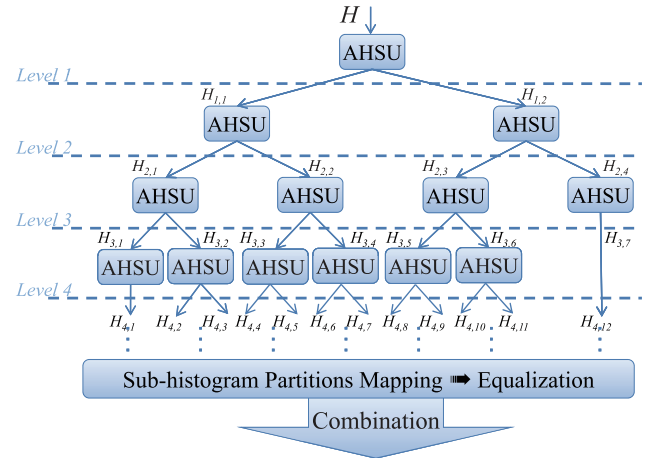


Fig. 1 Adaptive Histogram Separation and Mapping Framework (AHSMF).

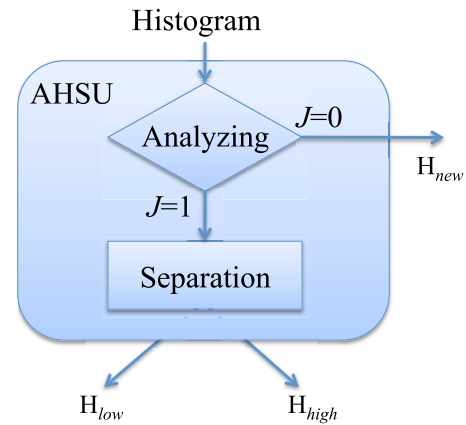


Fig. 2 Adaptive Histogram Separation Unit (AHSU).

### 2.1 Adaptive Histogram Separation Unit (AHSU)

AHSU is the key part of the proposed method, including the judgment part and separation part (Fig. 2).

**Separation Judgment:** To obtain the ideal automatic sub-histogram partitions, the first step is to judge whether the current sub-partition needs to be separated or not by AHSU is shown in Fig. 2. The following equations are used to determine whether it is flat or not in the local partition:

$$S(H_{i,j}) = H_{i,j}/255, \quad (1)$$

$$J = \begin{cases} 1 & \text{if } E\left(\left|\frac{\partial S(H_{i,j})}{\partial H_{i,j}}\right|\right) < Th, \text{ Separate} \\ 0 & \text{if } E\left(\left|\frac{\partial S(H_{i,j})}{\partial H_{i,j}}\right|\right) \geq Th, \text{ No separate} \end{cases} \quad (2)$$

In Eq. (2),  $Th$  is the threshold for judging and  $E\left(\left|\frac{\partial S(H_{i,j})}{\partial H_{i,j}}\right|\right)$  is the mean value of the modified histogram. If  $E(\cdot)$  is smaller than  $Th$ , then  $J = 1$  and the current partition must be separated, otherwise, the value is ignored. Based on considerable experiments and analysis using histogram partitions with 10 sample images,  $Th$  is fixed as 0.5. An example of separation judgment is shown in Fig. 3. In the histogram given in Fig. 3 (b), the yellow region looks flat, and the mean value is 1.0060 which is shown by the yellow line in Fig. 3 (c). The mean value of the yellow region is larger than  $Th$ , so there is no needs to separate it. However, the green region should be separated because that it includes peaks and valleys, and the mean value is 0.3214 as shown by the green

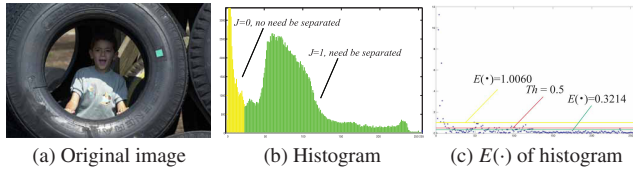


Fig. 3 Separation judgment example (image 2).

line in Fig. 3 (c).

**Separation point decision:** After judgment, the current partitions are separated by the separation point  $T$  which is defined as:

$$T = T_l + k(T_e - T_l), \quad (3)$$

where  $T_l$  is the separate point of the linear mapped histogram, and  $T_e$  is the separate point of the equalized histogram. Linear mapping enables the histogram to achieve a full range and keep the distribution global, whereas equalization allows the distribution of histogram to be obedient to probability. Here  $k$  is the controlling parameter. If  $k = 0$ , then Eq. (3) will be a linear separation point, whereas, if  $k = 1$ , then  $k$  is considered as an equalized point. The range of  $k$  is  $[0, 1]$ , providing the balance between the two extremes. After several tests,  $k = 0.8$  is used in our experiments. The separation point  $T_l$  in the histogram linear mapping is defined as:

$$T_l = \arg \max_{t_l} \{M_0(t_l)M_1(t_l) \cdot \|Av_0(t_l) - Av_1(t_l)\|^2\}, \quad (4)$$

where  $t_l$  is the current gray value,  $M_0(t_l)$  is the total number of the sub-histogram partitions, which is less than  $t_l$ , and  $M_1(t_l)$  is the total number of other partitions.  $Av_0(t_l)$  and  $Av_1(t_l)$  are the average of  $M_0(t_l)$  and  $M_1(t_l)$ , respectively. Separation point  $T_e$  in the equalized histogram is set as the middle point of the current partition.

After the separation judgment and separation point decision,  $J$  and  $T$  are used to split the histogram into two partitions as shown in Fig. 1. In the first level, AHSU is used to separate the original histogram into two sub-histogram partitions. And two AHSUs are used to process the two partitions. The process is repeated until the desired histogram is achieved. Finally,  $2^l - N$  sub-partitions are obtained at the  $l$ -th separation level, where  $N$  is the number of no separation sub-histogram partitions. Sometimes, one or two partitions can be separated more than 5 levels, but this situation is meaningless. So the maximum separation level is set to 4, which is obtained from mass experiments. The adaptive multi-level separation structure with 4-levels is shown in Fig. 1.

## 2.2 Exact Histogram Specification (EHS) [9]

However, obtaining the separate points in a normal histogram cannot provide accurate results because that one gray value may contain several pixels, which should be mapped to different new gray values. This separation cannot exactly solve the problem as it only maps one group of pixels with the same gray value to a new one. Therefore, EHS is used to obtain the exact histogram and redefine  $T_l$  as well as  $T_e$ .

The neighbor block based ordering is shown in Fig. 4. First, the gray levels are defined as  $G_i$ ,  $i \in [0, L]$ , 0 is the minimum

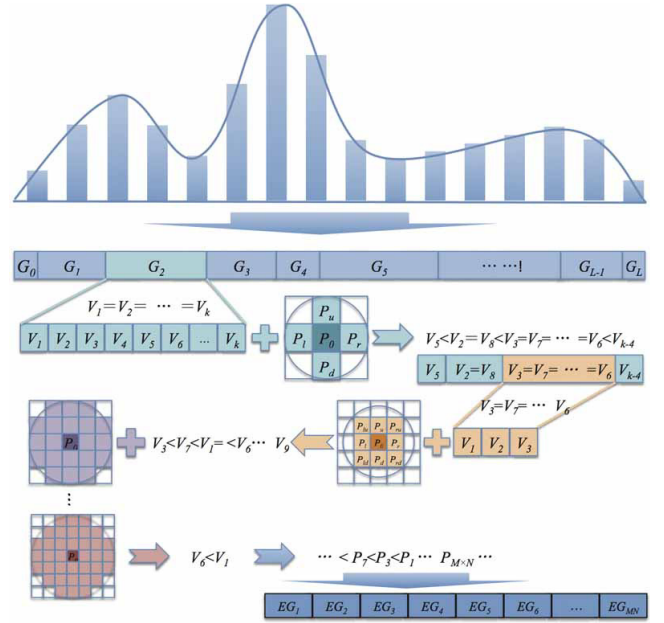


Fig. 4 Exact Histogram Specification.

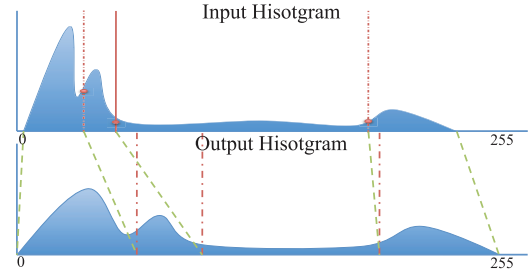


Fig. 5 Sub-histogram mapping.

value, and  $L$  is the maximum. If the image size is  $M \times N$ , then  $\sum_{i=0}^L G_i = M \times N$ . The pixels are then arranged according to gray values shown in Fig. 4. Here 255 is considered as a maximum value although many different pixels actually have the same gray value. To arrange equal pixels per group, 4 neighbor pixels with the current pixel are used to calculate the average value, demonstrated in Fig. 4 as  $G_2 = \{V_1, V_2, \dots, V_k\}$ ,  $V_1 = V_2 = \dots = V_k$ . Firstly,  $G_2$  pixels arranged by 4 neighbors mask, also neighbors 8, 20, and 36 are used to arrange  $G_i$  range at different levels to obtain the exact histogram.

Considering the concept of histogram equalization, the separation is not accurate because  $T_e$  must be the integer of gray value  $G$  in the original histogram. In EHS based histogram,  $T_e$  becomes the exact order of exact gray (EG) level. However, with EHS optimization, the separation becomes more accurate.

## 2.3 Sub-histogram Mapping

All sub-histogram partitions are mapped into a new range after separation. The order of separation points, calculated in the previous step as  $T_0, T_1, \dots, T_n$ , is shown as the red points in Fig. 5. These points are used to distill the sub-histogram partitions for mapping. If the range of sub-histogram partition is narrow and includes mass pixels, the histogram equalization method cannot obtain a good enhancement result. Therefore, the mapping function proposed in reference [1] is modified as follows:

$$H_{o_i} = T_i - T_{i-1}, \quad (5)$$

$$factor_i = H_{o_i} \times (\log M_i)^C, \quad (6)$$

$$C = \log[E(I)], \quad (7)$$

$$H_{m_i} = \frac{factor_i \times 255}{\sum_{k=0}^n factor_k}, \quad (8)$$

where  $H_{o_i}$  is the original sub-histogram partition separated by  $T_i$ , and  $T_{i-1}$ .  $T_i$  is the  $i$ -th threshold of the input histogram partition,  $M_i$  is the number of all pixels of  $i$ -th sub-histogram partition, where  $factor_i$  is the zoom factor of the  $i$ -th sub-histogram partition,  $C$  is the brightness factor, and  $H_{m_i}$  is the mapped sub-histogram partition.

### 2.4 Sub-histogram Partitions Equalization

The partitions are equalized independently after mapping. For sub-histogram partition  $i$  ( $i \in [1, 2^l - N]$ ), equalization starts from  $Start_i$  and ends at  $End_i$ . Therefore, equalization aims to  $[Start_i, End_i]$  partition by the following equation:

$$y(g) = Start_i + (End_i - Start_i) \sum_{k=Start_i}^g \frac{n_k}{M}, \quad (9)$$

where  $n_k$  is the number of pixels with intensity  $k$ ,  $M$  is the total pixels contained in partition  $H_i$ , and  $g$  is the current gray value,  $g \in [Start_i, End_i]$ . If  $Start_i = 0$  and  $End_i = 255$ , Eq. (9) is the same as the global HE.

After global enhancement, the whole image is enhanced to a natural looking image. However, the histogram adjustment method has some drawbacks because it only captures the display contract when it exceeds the linear tone mapping operator. Further refinement is performed by human contract. The whole image is enhanced but some details are not clear enough. So the neighbor block based local operator will be used to address this issue.

## 3. Local Neighbor Optimization

Since that the details of image cannot be enhanced by global methods, we focus on local region analysis and optimization method in this section. Generally speaking, local enhancement affects the artifact. Therefore, local block neighbor weight optimization method is used to overcome the problem and it can achieve better result for display.

### 3.1 Local Operator

To obtain a fast local operator, the image is simply divided into non-overlapping regular rectangular blocks. To achieve this condition, the block size is considered as well as local contrast enhancement method.

In order to fix the size of blocks, the block sizes, from  $200 \times 200$ ,  $100 \times 100$ ,  $\dots$ , to  $10 \times 10$ , were tested and compared. Given that the total pixels of the local block are not sufficient, the global method is used directly for more effective analysis. A  $30 \times 30$  and local contrast enhancement method e.g., EHS is used after comparing the global methods HE and EHS with different block sizes. However, the enhanced images have obvious boundary artifacts.

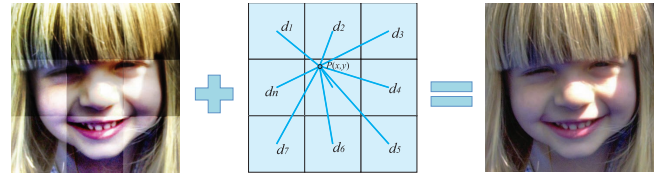


Fig. 6 Neighbor Weighting based Boundary Artifact Removal.

### 3.2 Neighbor Weighted based Boundary Artifact Removal [10]

To eliminate the boundary artifacts, an approach is introduced and illustrated in Fig. 6. For each pixel  $P(x, y)$  in the image, the final mapped pixel value is the weighted average of the results from block based EHS according to a distance weighed function as follows:

$$d(x, y) = \frac{\sum_{n=1}^{n=k} EHS_n[P(x, y)] \cdot \sigma_d(n)}{\sum_{n=1}^{n=k} \sigma_d(n)}, \quad (10)$$

where the distance weight function  $\sigma_d$  is calculated by

$$\sigma_d(n) = e^{-d_n/\sigma_d}, \quad (11)$$

and  $d_n$  is the Euclidean distance between the current pixel position and the center of each blocks shown in Fig. 6,  $\sigma_d$  controls the smoothness of the image. The boundary smoothing factor  $\sigma_d$  to larger values can make an image free from boundary artifacts with less local contrast. Setting  $\sigma_d$  to smaller values makes the smoothing less obvious and the resulted image shows more local contrast but boundary artifacts are emerged as well. The block size is set to 20 to show good results, which not only smoothens the boundary artifacts but also preserves the local contrast.  $K$  is the block number used in the weighted operation. Here setting  $\sigma_d$  as 20 enables  $5 \times 5$  neighborhood blocks to work well. Therefore, the sum in Eq. (9) is only over 25 blocks, i.e.,  $K = 25$ .

The images after considering the distance weighting function are shown in Fig. 6. Good results are obtained and the disturbing boundary artifacts are eliminated. Thus, these images show details and local contrast as well as a more natural appearance.

## 4. Experimental Results and Discussion

In this section, the performance of the proposed method and the comparison with state-of-art approaches will be discussed. The test sample images are got from NASA Langley Research Center, and all experiments are tested using Matlab on Mac PC with 2.4 GHz CPU and 4 Gb memory. The image size is  $2000 \times 1300$ . It takes about 3 seconds for processing.

Here, we present the results of the image set with other methods: HE, dynamic HE (DHE) [1], alpha rooting (AR) [4], RMSHE [6], GLG [8], EHS [9], color enhancement by scaling (CES) [15], multi-contrast enhancement (MCE) [22], and contrast normalization (CN) [24]. The names of different methods and the parameter setting used in experimentations are listed in Table 1.

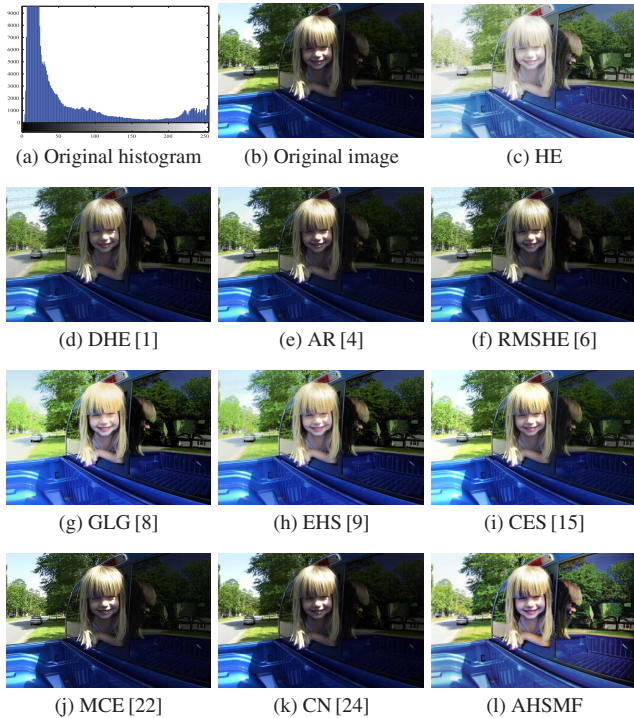
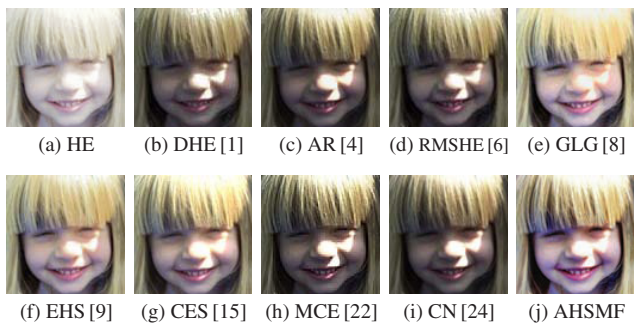
### 4.1 Subject Comparison

In the comparison of Fig. 7, CES looks most natural, however the sky and ground are a little bright. Though the HE makes the

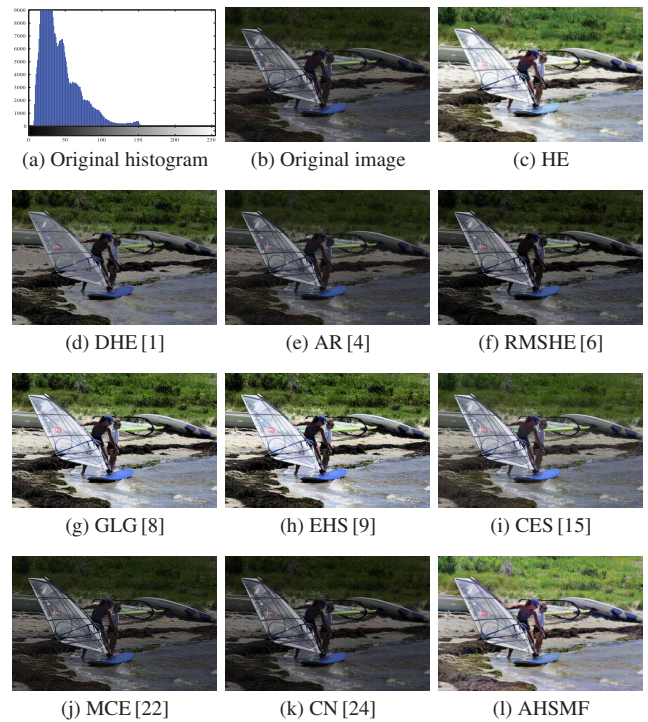
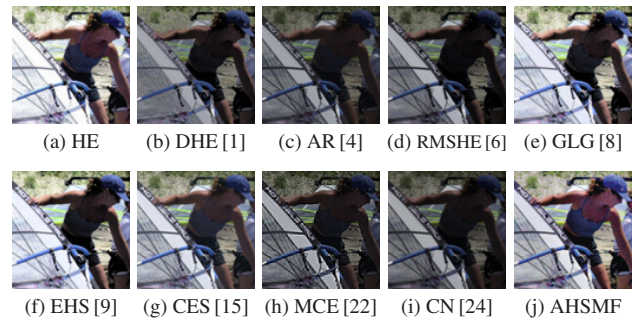


**Table 1** List of enhancement methods.

Enhancement Method	Short Name	Parameters
Histogram Equalization	HE	Automatic
Dynamic Histogram Equalization [1]	DHE	Automatic
Alpha Rooting [4]	AR	$\alpha = 0.98$
Recursive Mean-Separate HE [6]	RMSHE	$r = 2$
Gray-Level Grouping [8]	GLG	Automatic
Exact Histogram Separation [9]	EHS	Automatic
Color Enhancement by Scaling [15]	CES	$B_{max} = 255$ $k = 1.0$ $\delta_{thresh} = 15$
Multi-Contrast Enhancement [22]	MCE	$\lambda = 1.95$
Contrast Normalization [24]	CN	$\mu_c = 0$
Adaptive Histogram Separation and Mapping Framework	AHSMF	Automatic


**Fig. 7** Result comparison with image 16.

**Fig. 8** Local result comparison with image 16.

dark region clear, the bright region also become brighter, and the color of car and face are not correct. GLG is better than HE, and looks the same as the EHS and CES, but some regions have halo effect. For the contrast, EHS looks better, however the class region is also a little dark and the sky region becomes a little unnatural. Compared with other methods, the proposed AHSMF enhances the detail in dark and bright region ideally, however the color does not look natural enough. Also, in the local compari-


**Fig. 9** Result comparison with image 18.

**Fig. 10** Local result comparison with image 18.

son as **Fig. 8** shown, the HE is too bright and others look better, and the color in the proposed method, shows better effective than other methods.

In **Fig. 9**, the results of HE, GLG, EHS, CES, and AHSMF are acceptable. However, the sailboat of HE is too bright to observe some details, the face and coast in EHS are too dark to see. The details of GLG and CES are look well, but the whole image is not bright and clear enough. The proposed AHSMF shows the details in all kinds of region and better global vision effect. As the local region of the person (**Fig. 10**), the EHS is a little darker, CES, HE, and AHSMF are better. However, for the sailboat we can see that the result of HE is too bright, so CES and the proposed method are the best.

In **Fig. 11**, the effects of HE, GLG, and EHS look the same, the CES is a little darker but shows more details in bright region. However, in the dark region, the car and the details of tree are difficult to be observed. The proposed AHSMF can overcome this problem and show the detail in both kinds of region ideally. In order to further compare the details, **Fig. 12** makes a good comparison. In the local region HE looks too bright, GLG and EHS are better than HE, however both two methods cannot show some



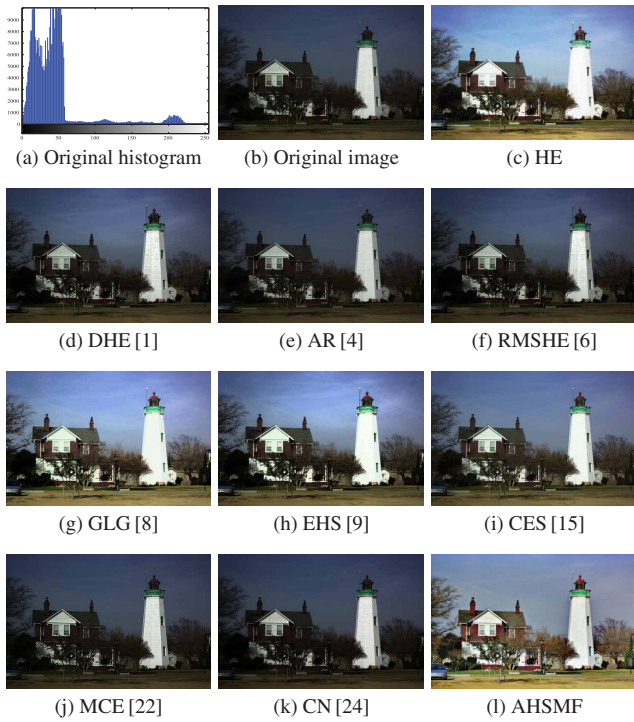


Fig. 11 Result comparison with image 22.

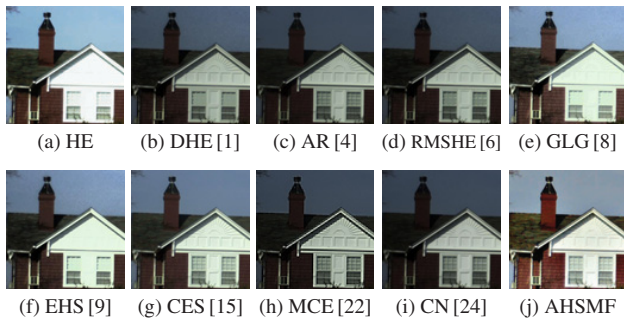


Fig. 12 Local result comparison with image 22.

details of house. For the white region of house, CES is a little better than AHSMF, but for the dark region the proposed AHSMF is better than CES.

In Fig. 13, despite the building of CES looks good, the whole image turns dark and the details of tree are difficult to be observed. Unlike the CES, the dark region in the result of HE turns out to be good, but the buildings are too bright. And in vision, GLG and EHS look better than AHSMF, but some details are not clear enough, such as the tree and brick of wall. Also, as the local region comparison shown in Fig. 14, proposed AHSMF shows better effectiveness in bright and dark region than other methods.

After these comparisons, the proposed AHSMF looks better than other referenced methods. However, this kind of research is hard to find a criterion to evaluate objectively, because that the real images are not existed. So we invite 20 persons to observe the results and make the score with the effect of vision including the whole image, contrast, and details, where full mark is set as 5, 2.5, and 2.5, respectively. The total score (full mark as 10) is shown in Fig. 15. From this comparison, we can see that the proposed method is better than other reference methods.

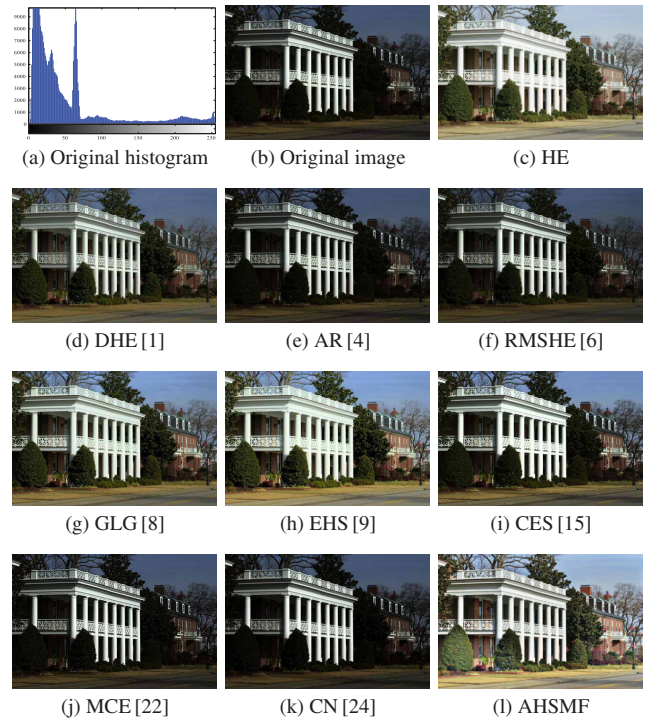


Fig. 13 Result comparison with image 23.

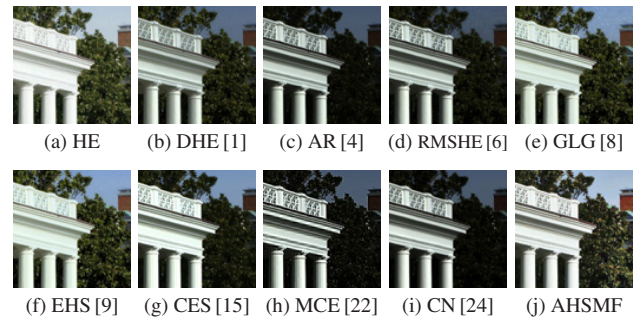


Fig. 14 Local result comparison with image 23.

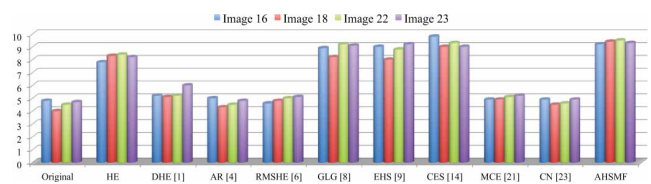


Fig. 15 Score of example images by subjective vision.

## 4.2 Objective Comparison

The quality of Image enhancement is difficult to be evaluated. Among all enhancement methods, better one should provide more features. And for comparing different methods, objective comparison is hardly evaluated, because no original image exists. Here, we make the ideal original images artificially, which get score 10 in subjective comparisons. In this section, the widely used measures include the absolute mean brightness error (AMBE) [5], [7], [12], different image entropy (DIE), peak signal to noise ratio (PSNR), edge overlapping ratio (EOR) [23], mean segmenting overlapping ratio (MSOR) [23] will be introduced and compared. These measures can get the objective score for comparison and described as follows.

#### 4.2.1 Absolute Mean Brightness Error (AMBE)

AMBE is absolute difference between the mean of input and output images. The measure equation is given as follows:

$$AMBE = |E(I_{in}) - E(I_{out})|, \quad (12)$$

where  $E(I_{in})$  is the average intensity of the input image and  $E(I_{out})$  is the average intensity of the output image. The smaller AMBE value shows that the average intensity of the input and output image are more equal.

#### 4.2.2 Different Image Entropy (DIE)

The entropy is used to measure the content of an image, where a higher value indicates an image with richer details. Also, for comparing the details with two images, the following equation is used:

$$DIE = \sum_{i=0}^{L-1} |P_{in}(i) \log_2 P_{in}(i) - P_{out}(i) \log_2 P_{out}(i)|, \quad (13)$$

where  $P(i)$  is the probability of  $i$ -th gray value, the  $P_{in}$  and  $P_{out}$  are the probability of the enhanced image and original low contrast image.

#### 4.2.3 Peak Signal to Noise Ratio (PSNR)

PSNR is widely used to compare the quality of two images in many regions, such as image compression, denoising, etc. So to describe the intensity changes of the input and output images, PSNR can be used to measure it by:

$$PSNR = 10 \log_{10} \left( \frac{255^2}{MSE} \right), \quad (14)$$

where MES is the mean square error which defined as:

$$MSE = \frac{1}{mn} \sum_{i=0}^{m-1} \sum_{j=0}^{n-1} \|I_{in}(i, j) - I_{out}(i, j)\|^2, \quad (15)$$

where  $m$  and  $n$  are the width and height of image.

#### 4.2.4 Edge Overlapping Ratio (EOR)

Considering the edge is important to an image, so the EOR can be used to measure the edge information. First do edge detection by same parameter settings on both input image  $I_{in}$  and output image  $I_{out}$  to get two edge images. Then binary the two edge images  $I'_{in}$  and  $I'_{out}$  where edge pixels as 1 and other pixels as 0. Finally, using the following equation to calculate EOR:

$$EOR = \frac{|I'_{in} \cap I'_{out}|}{|I'_{in}| + |I'_{out}| - |I'_{in} \cap I'_{out}|}, \quad (16)$$

where  $|\cdot|$  denotes the number of edge pixels. The EOR more close to 1, means the edge of two images more close.

#### 4.2.5 Mean Segmenting Overlapping Ratio (MSOR)

Since automated interpretation benefits from image enhancement, it can also be used as an important goal for image enhancement. Here MSOR is used to measure for this task. Suppose  $I_{in}$  has  $M$  segments  $A = a_1, a_2, \dots, a_m$  and  $I_{out}$  has  $N$  segments  $B = b_1, b_2, \dots, b_n$  by same segmentation algorithm. How to depict the similarity between them is not easy since the number of segments may be different. Inspired the number by the definition of Hausdorff distance for point set matching, MSOR is here defined as:

**Table 2** Result comparison (average of 20 color images).

Method	AMBE	DIE	PSNR	EOR	MSOR
Original	49.959	0.464	15.385	0.345	0.318
HE	25.779	0.595	14.797	0.394	0.410
DHE [1]	20.331	0.486	19.983	0.449	0.433
AR [4]	23.031	0.486	17.701	0.489	0.412
RMSHE [6]	23.137	0.488	17.705	0.496	0.421
GLG [8]	20.003	0.415	20.821	0.524	0.456
EHS [9]	20.088	0.422	21.838	0.542	0.459
CES [15]	16.046	0.442	20.648	0.553	0.465
MCE [22]	23.124	0.498	17.712	0.512	0.426
CN [24]	23.413	0.489	17.695	0.501	0.422
AHSMF	15.004	0.460	22.456	0.562	0.471

$$MSOR(A, B) = \frac{1}{M} \sum_{a \in A} \rho(a, B), \quad (17)$$

where  $\rho(a, B)$  is the maximum ratio of a segment  $b$  in  $B$  overlapped with segment  $a$ :

$$\rho(a, B) = \max \left( \frac{|a \cap b|}{|a| + |b| - |a \cap b|} \right), \quad (18)$$

where  $|\cdot|$  means the number of pixels in a segment. The MSOR can describe the similarity of two segments sets.

#### 4.2.6 Objective Evaluation

To make the objective comparison and conclusion, the evaluation criterion introduced previously are used. **Table 2** shows the average score of 20 sample images with HE, DHE, AR, RMSHE, GLG, EHS, CES, MCE, CN, and proposed AHSMF by AMBE, DIE, PSNR, EOR, and MSOR. For AMBE and DIE, smaller score means better. And for PSNR, EOR and MSOR, larger score mean the enhanced image more close to ideal image. From comparison, it is easily to conclude that the proposed AHSMF method can get better result for low contrast images.

## 5. Conclusion

This paper presents a framework with adaptive histogram separation and mapping strategy as a new image enhancement method. The proposed method can obtain good results with visually pleasing, artifact free, and natural looking both in dark and light region with narrow histogram range image. The experimental results show the effectiveness of the proposed method in comparison to other contrast enhancement algorithms.

**Acknowledgments** We would like to thank the reviewers for some very helpful comments on the original vision of the manuscript and all people providing their free coed and test image for this study. We also thank Can Tong, Pengyi Hao, and Wei Zhou for their discussion to improve the paper.

## References

- [1] Abdullah-Al-Wadud, M., Kabir, M., Dewan, M. and Chae, O.: A Dynamic Histogram Equalization for Image Contrast Enhancement, *IEEE Trans. Consumer Electronics*, Vol.53, No.2, pp.593–600 (2007).
- [2] Agaian, S., Panetta, K. and Grigoryan, A.: Transform-based Image Enhancement Algorithms with Performance Measure, *IEEE Trans. Image Processing*, Vol.10, No.3, pp.367–382 (2001).
- [3] Agaian, S., Silver, B. and Panetta, K.: Transform Coefficient Histogram-based Image Enhancement Algorithms Using Contrast Entropy, *IEEE Trans. Image Processing*, Vol.16, No.3, pp.741–758 (2007).
- [4] Aghagolzadeh, S. and Ersoy, O.: Transform Image Enhancement, *Optical Engineering*, Vol.31, pp.614–626 (1992).
- [5] Arici, T., Dikbas, S. and Altunbasak, Y.: A Histogram Modification Framework and Its Application for Image Contrast Enhancement,



- IEEE Trans. Image Processing*, Vol.18, No.9, pp.1921–1935 (2009).
- [6] Chen, S. and Ramli, A.: Contrast Enhancement Using Recursive Mean-Separate Histogram Equalization for Scalable Brightness Preservation, *IEEE Trans. Consumer Electronics*, Vol.49, No.4, pp.1301–1309 (2003).
  - [7] Chen, S. and Ramli, A.: Minimum Mean Brightness Error Bi-Histogram Equalization in Contrast Enhancement, *IEEE Trans. Consumer Electronics*, Vol.49, No.4, pp.1310–1319 (2003).
  - [8] Chen, Z., Abidi, B., Page, D. and Abidi, M.: Gray-Level Grouping (GLG): An Automatic Method for Optimized Image Contrast Enhancement – Part I: The Basic Method, *IEEE Trans. Image Processing*, Vol.15, No.8, pp.2290–2302 (2006).
  - [9] Coltuc, D., Bolon, P. and Chassery, J.-M.: Exact Histogram Specification, *IEEE Trans. Image Processing*, Vol.15, No.5, pp.1143–1152 (2006).
  - [10] Duan, J., Bressan, M., Dance, C. and Qiu, G.: Tone-mapping High Dynamic Range Images by Novel Histogram Adjustment, *Pattern Recognition*, Vol.43, No.5, pp.1847–1862 (2010).
  - [11] Han, J., Yang, S. and Lee, B.: A Novel 3-D Color Histogram Equalization Method with Uniform 1-D Gray Scale Histogram, *IEEE Trans. Image Processing*, Vol.20, No.2, pp.506–512 (2011).
  - [12] Ibrahim, H. and Kong, N.: Brightness Preserving Dynamic Histogram Equalization for Image Contrast Enhancement, *IEEE Trans. Consumer Electronics*, Vol.53, No.4, pp.1752–1758 (2007).
  - [13] Kim, J., Kim, L. and Hwang, S.: An Advanced Contrast Enhancement Using Partially Overlapped Sub-Block Histogram Equalization, *IEEE Trans. Circuits and Systems for Video Technology*, Vol.11, No.4, pp.475–484 (2001).
  - [14] Kim, T. and Yang, H.: A Multidimensional Histogram Equalization by Fitting an Isotropic Gaussian Mixture to a Uniform Distribution, *IEEE Int'l Conf. on Image Processing (ICIP'06)*, pp.2865–2868 (2006).
  - [15] Mukherjee, J. and Mitra, S.: Enhancement of Color Images by Scaling the DCT Coefficients, *IEEE Trans. Image Processing*, Vol.17, No.10, pp.1783–1794 (2008).
  - [16] Nilsson, M., Dahl, M. and Claesson, I.: Gray-Scale Image Enhancement Using the SMQT, *IEEE Int'l Conf. on Image Processing (ICIP'05)*, Vol.1, pp.1–933–6 (2005).
  - [17] Pei, S., Zeng, Y. and Ding, J.: Color Images Enhancement Using Weighted Histogram Separation, *IEEE Int'l Conf. on Image Processing (ICIP'06)*, pp.2889–2892 (2006).
  - [18] Pizer, S., Ambum, E., Austin, J., Cromartie, R., Geselowitz, A., Greer, T., Romeny, B., Zimmerman, J. and Zuiderveld, K.: Adaptive Histogram Equalization and Its Variations, *Computer Graphics and Image Processing*, Vol.39, No.4, pp.355–368 (1987).
  - [19] Sen, D. and Pal, S.: Automatic Exact Histogram Specification for Contrast Enhancement and Visual System Based Quantitative Evaluation, *IEEE Trans. Image Processing*, Vol.20, No.5, pp.1211–1220 (2011).
  - [20] Stark, J.: Adaptive Image Contrast Enhancement Using Generalizations of Histogram Equalization, *IEEE Trans. Image Processing*, Vol.9, No.5, pp.889–896 (2000).
  - [21] Greenspan, H., Anderson, C.H. and Akber, S.: Image Enhancement by Nonlinear Extrapolation in Frequency Space, *IEEE Trans. Image Processing*, Vol.9, No.6, pp.1035–1048 (2000).
  - [22] Tang, J., Peli, E. and Acton, S.: Image Enhancement Using a Contrast Measure in the Compressed Domain, *IEEE Signal Processing Letter*, Vol.10, No.10, pp.289–292 (2003).
  - [23] Tian, L. and Kamata, S.: Image Enhancement by Analysis on Embedded Surfaces of Images and a New Framework for Enhancement Evaluation, *IEICE Trans. Information and Systems*, Vol.E91-D, No.7, pp.1946–1954 (2008).
  - [24] Veldkamp, W. and Karssemeijer, N.: Normalization of Local Contrast in Mammograms, *IEEE Trans. Medical Imaging*, Vol.19, No.7, pp.731–738 (2000).
  - [25] Zhang, Q., Inaba, H. and Kamata, S.: Adaptive Histogram Analysis for Image Enhancement, *Pacific-Rim Symp. on Image and Video Technology (PSIVT'10)*, pp.408–413 (2010).



**Qieshi Zhang** is a Ph.D. student of the Graduate School of Information, Production and Systems, Waseda University, Japan, where he received his M.E. degree in 2009. He received his B.E. degree major in Automation and minor in Computer and Application from the Faculty of Automation and Information Engineering,

Xian University of Technology, China in 2004. From 2004 to 2006, he was an assistant engineer of the Department of Mechanical Electronically Technology in Xi'an Siyuan University, China. From 2009 to 2010, he was a teaching assistant in the Graduate School of Information, Production and Systems, Waseda University. From 2010 to 2012, he was a Research Fellow of the Japan Society for the Promotion of Science (JSPS), Japan. His current research interests are in image processing, image compression, image detection, image enhancement, pattern recognition, machine learning, and computer vision. He is a student member of the IEEE and IEICE.



**Sei-ichiro Kamata** received his M.S. degree in computer science from Kyushu University, Fukuoka, Japan, in 1985, and Doctor of Computer Science, Kyushu Institute of Technology, Kitakyushu, Japan, in 1995. From 1985 to 1988, he was with NEC, Ltd., Kawasaki, Japan. In 1988, he joined the faculty at Kyushu Institute of

Technology. From 1996 to 2001, he has been an associate professor in the Department of Intelligent System, Graduate School of Information Science and Electrical Engineering, Kyushu University. Since 2003, he has been a professor in the Graduate School of Information, Production and Systems, Waseda University. In 1990 and 1994, he was a Visiting Researcher at the University of Maine, Orono. His research interests include image processing, pattern recognition, image compression, and space-filling curve application. He is a member of IEEE, IEICE, IPSJ, IIEEJ and ITE in Japan.

(Communicated by Yasuyuki Matsushita)